Submicron-Lubricant Based on Crystallized Fe_3O_4 Spheres for Enhanced Tribology Performance

Xiaoyun Song,[†] Zhiwen Qiu,[†] Xiaopeng Yang,[†] Haibo Gong,[†] Shaohua Zheng,[†] Bingqiang Cao,*[,†] Hongqiang Wang, *[,‡] Helmuth Moehwald,[‡] Dmitry Shchukin[§]

[†] Laboratory of Inorganic Functional Materials in Universities of Shandong, School of Material Science and Engineering, University of Jinan, Jinan 250022, China

[‡] Department of Interfaces, Max Planck Institute of Colloids and Interfaces, Potsdam-Golm, 14424, Germany

[§] Stephenson Institute for Renewable Energy, Department of Chemistry, University of Liverpool, Peach Street, Liverpool, L69 7ZF, UK

Supporting Information

ABSTRACT: We demonstrate in this paper a novel finding of submicron-lubricant exemplified by crystallized magnetite (Fe_3O_4) submicrometer spheres. Optimized tribological performance of lubricant particles occurs when the particles are submicrometer sized and spherical. The tribology of lubricant particles is thus verified to be size and shape dependent. Owing to the unique heating and quenching process involved in pulsed laser irradiation, Fe_3O_4 submicrometer spheres are acquired through phase transformation and reshaping. The formation process of the regular Fe_3O_4 spheres in deionized water was investigated by choosing different laser fluences and irradiation times. The shape and phase transformation mechanisms are elucidated as well. Tribological properties of the obtained Fe_3O_4 submicrometer spheres have been explored, inspired by their spherical shape and smooth surfaces. Crystallized magnetite submicrometer spheres under optimized conditions show a reduction in friction and wear by up to 40% and 20%, respectively. Control experiments revealed that nanoparticles, non-spherical submicrometer particles and micrometer particles could not reach such good tribology performance, indicating the potential of adopting crystallized Fe_3O_4 submicrometer spheres in the application of mechanical energy saving.

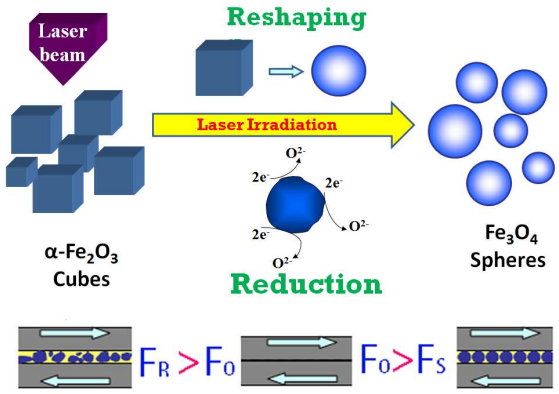

1. INTRODUCTION

The ability to generate micro/nanocrystals with well-controlled sizes, shapes, and compositions is central to advance applications ranging from catalysis to electronics, photonics, sensing, as well as energy generation, storage, and conversion.[1-5] Developing nanostructures with designed morphologies for investigation of tribology has recently been of importance as one third of the total mechanical energy used in this world goes waste to counteract the friction force.[6-8] Nanoparticles including ZnO[6,8] and Al_2O_3[7] have shown good potential as additives for lubricant to improve its tribology property. Intriguingly, earth abundant Fe_2O_3 and Fe_3O_4 are more attractive for such applications when considering their high hardness (1030 and ~450 Hv, respectively). Attempts have been thus reported by using iron oxides as additives in base oil in the form of micro/nanoparticles.[9] Numerous methods have been developed for the synthesis of high-quality iron oxide nanoparticles, such as precursor-templated methods,[10] hydrothermal methods,[11] and chemical precipitation.[12] However, the morphologies of nanoparticles prepared by the above methods are usually non-spherical.[13-15]

In addition, research related to the particles based lubricant has always focused on seeking ideal material species,[6-15] while few on the investigation of size-dependent tribology properties, which is of importance not only fundamentally but for practical application.

In view of the primary principles of lubrication, spherical particles with high hardness are highly appreciated to change sliding into rolling friction more effectively and reduce the wear more significantly. No efforts, however, to the best of our knowledge, have been reported on spherical iron oxides particles for lubrication. As a matter of fact, synthesis of iron oxide particles with spherical shape has been well documented in literatures, however, the acquired particles are dominated by hierarchical structures, i.e. the spherical particles are constructed by secondary subunits.[13] As aforementioned above, these particles are not ideal as well for lubricating when considering their surface roughness and low hardness. Unfortunately, synthesis of inorganic highly crystalline spheres with smooth surfaces has rarely been reported, possibly because of their very high melting points and anisotropic crystal structures.

Laser ablation has recently been adopted to synthesize particles both in vapor or liquid medium, which is known as pulsed laser ablation (PLA). The combination of laser ablation and vapor transport deposition provide good control over the temperature, pressure and gas to grow nanostructures, especially for one-dimensional nanowires or nanotubes.[16-19] Laser ablation in liquid media was firstly implemented to fabricate colloidal solutions of nanoparticles, known as laser ablation in liquid (LAL).[20, 21] Henglein et al. [22] first applied a pulsed laser to ablate pure metal targets in various solvents to grow colloidal solutions containing metal nanoparticles (NPs). Since then, LAL has been deeply developed as an important method to prepare metal, semiconductor, and even polymer NPs.[23-25] For instance, Zeng et al.[26-28] reported composition-controlled synthesis of ZnO-Zn composite nanoparticles by laser ablation of a zinc metal target in pure water and aqueous solution of sodium dodecyl sulfate and studied their optical properties; Yang et al.[29, 30] have synthesized Si quantum dots and SiC quantum rings using LAL and an anomalous quantum confinement effect was observed; Jayawardena et al.[30] showed that ZnO nanocrystals and nanorods can be fabricated by hybrid hydrothermal and UV laser heating growth process.

Most recently, metal and semiconductor submicrometer spheres have been prepared by a selective pulsed laser heating process with proper laser wavelength and energy,[32, 33] which effectively inhibits the anisotropic crystal growth and favors for acquiring inorganic crystalline spheres. Inspired by this, in this manuscript, we introduce crystalline Fe_3O_4 submicrometer spheres for lubrication by simple pulsed laser irradiation of preformed α-Fe_2O_3 cubic particles. A laser-stimulated surface tension energy release (LSTER) and chemical phase transition process involved in the laser irradiation process assures the formation of spherical Fe_3O_4 particles. What is more important, the lubrication of iron oxide NPs, cubic submicrometer particles and microparticles was further investigated, verifying a novel phenomenon of "sub-micron-lubricant", i.e. crystalline submicrometer spheres exhibiting superior tribology performance.

2. EXPERIMENTAL SECTION

2.1 Synthesis of hematite (Fe_2O_3) cubic particles. Fe_2O_3 cubic particles were prepared by a hydrothermal process. In a typical reaction, 0.729 g CTAB, 0.622 g $FeCl_3\,6H_2O$ and 0.4 g PEG-6000 was dissolved into 60 ml deionized water. The whole mixture was stirred to form a homogeneous solution and then transferred into a Teflon-lined stainless steel autoclave. Then it was sealed and maintained at 120 ℃ for 12 h. After the reaction, the precipitated powders were collected by centrifuging and washed several times with deionized water and ethanol. Finally, the samples were dried at 50 ℃ for 12 h.

2.2 Synthesis of magnetite submicrometer spheres. The as-prepared Fe_2O_3 cubic particles were dispersed into deionized water at a mass concentration of 0.5 wt% to form a colloidal solution. A KrF excimer laser (10 Hz, 25 ns, Coherent, CompexPro 205) was used as the light source for pulsed laser irradiation. The pulsed laser beam was guided by a reflection mirror and focused by a quartz lens on colloidal solution. The solution was then irradiated with a focused laser beam with different laser fluences (400, 700, 1000, 1300 mJ $pulse^{-1}$ cm^{-2}), which were determined by a laser FieldMaxII Meter (Coherent). Laser irradiation of raw Fe_2O_3 particles was performed for different times. After laser irradiation, all prepared colloidal suspensions were centrifuged at 8000 rpm and finally dried at 50 ℃ for further characterization.

2.3 Structure and tribology characterizations. The sample morphology was characterized with a scanning electron microscope (SEM, FEI Quanta 250 FEG). The phase and crystal structures of the particles were investigated with X-ray diffraction (XRD, Cu Kα radiation, Bruker D8 ADVANCE) and X-Ray photoelectron spectroscopy (XPS, ThermoFisher, ESCALAB 250). The tribological properties of the prepared particles were measured in terms of friction coefficients and wear scar diameters with a tribology tester (MMU-10G, Sinomach-Jinan). Fe_3O_4 submicrometer spheres dispersed into oil with different mass concentration of 0, 0.03, 0.07, 0.13, and 0.2 wt%, respectively, were tested. Control experiments were performed by measuring the tribological properties of as-prepared α-Fe_2O_3 cubic particles, magnetite nanoparticles, hierarchical magnetite spherical particles with 0.03 ~0.2 wt%. Detailed experimental conditions of the four-ball wear test were set as follows: rotation speed at 1450 r/min, load of 147 N, temperature at 75 ℃ and time of 30 min. The friction coefficient was recorded *in situ* and the test data were acquired automatically with a computer. The size of the wear scar diameter was observed with a metallographic microscope and then the average size of wear scar diameter was obtained.

3. RESULTS AND DISCUSSIONS

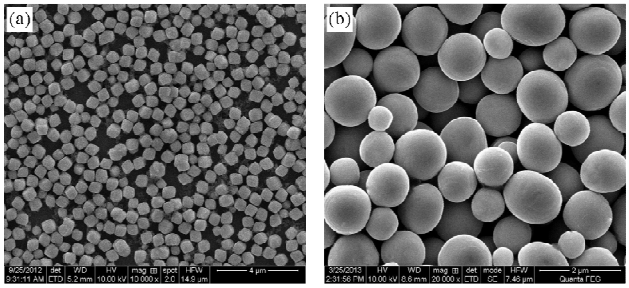

Figure 1. SEM images of (a) nanoparticles prepared by hydrothermal method and (b) submicrometer spheres after irradiation with a 248 nm KrF excimer laser for 60 min under fluence of 1300 mJ pulse^{-1} cm^{-2}.

3.1 Morphology and phase analysis of Fe_3O_4 submicrometer particles. Figure 1(a) shows a typical SEM image of as-prepared particles synthesized by a hydrothermal method, from which it can be seen that the particles are cubic with edge length of about 600 nm. After UV laser irradiation for 55 min with fluence of 1300 mJ pulse^{-1} cm^{-2} in deionized water, these cubes transform to submicrometer spheres as shown in Figure 1(b). One can note that the size of the spherical particles after laser irradiation is similar to or a little bigger than that of the corresponding raw cubic particles. This is totally different from the case of traditional LAL that a solid or pressed target is laser ablated in liquid, which usually produces much smaller particles with size of a few nanometers.[10] The composition and phase purity of the particles with different morphologies were further examined by XRD, as shown in Figure 2(a). The XRD pattern of the as-prepared cubic samples can be well ascribed to the rhombohedral α-Fe_2O_3 (PDF: 24-0072,). However, after laser irradiation, the XRD pattern of the submicrometer spheres exhibits different diffraction characteristics. By comparing the XRD peaks with the standard powder diffraction cards, the submicrometer spheres can be identified as the γ-Fe_2O_3 (PDF: 24-0081)[34] or Fe_3O_4 (PDF: 89-4319).

XPS measurement was employed to check the phase change upon laser irradiation due to its sensitivity to surface chemical changes. Figure 2(b) shows the wide scanning spectrum and the photoelectron peaks at binding energies of about 710.8, 530.8 eV and 285.0 eV, which is attributed to Fe2p, O1s and C1s, respectively.[15] Figure 2(c) shows the XPS signals of the Fe2p peak, with two peaks of $Fe2p_{1/2}$ at 710.8 eV and $Fe2p_{3/2}$ at 724.0 eV with the full width at half-maximum (FWHM) of 4.1 and 5.1 eV, respectively. The absence of the satellite peak situated at about 719 eV, which is a major characteristics of Fe^{3+} in γ-Fe_2O_3, clearly excludes the formation of γ-Fe_2O_3 after laser irradiation.[35] The O core level spectrum together with their spectral deconvolution curves in Figure 2(d) consists of a main peak originating from the oxygen in Fe_3O_4 (at 530.0 eV) and a shoulder centered at 531.4 eV, which is ascribed to surface traps.[36] Moreover, the total Fe/O ratio was estimated to be 0.74 by curve resolution analysis, which is well consistent with the stoichiometric ratio of Fe_3O_4. The XPS and XRD analysis reveal that the raw cubic particles are rhombohedral α-Fe_2O_3, and spinel Fe_3O_4 submicrometer spheres are obtained after pulsed laser irradiation. Therefore, the physical reshaping and phase transition from α-Fe_2O_3 cubes to Fe_3O_4 spheres are induced by a simple laser irradiation process in water. Compared with the conventional chemical routes, this method is very fast, moderate, and safe, and does not use any surfactants.[26, 32] To disclose more details about the morphology evolution, irradiation time-dependent and laser energy-dependent experiments were further conducted.

3.2 Effect of laser fluence and irradiation time on particle shape Figure 3 shows SEM images of the prepared Fe_3O_4 particles. When the laser fluence is as low as 0.4 J pulse^{-1}cm^{-2}, the par- ticles do not show clear morphological changes, but only few small spherical particles are formed, as shown in Figure 3(a). This is because the laser cannot produce enough energy to melt the particle surfaces. When the laser fluence

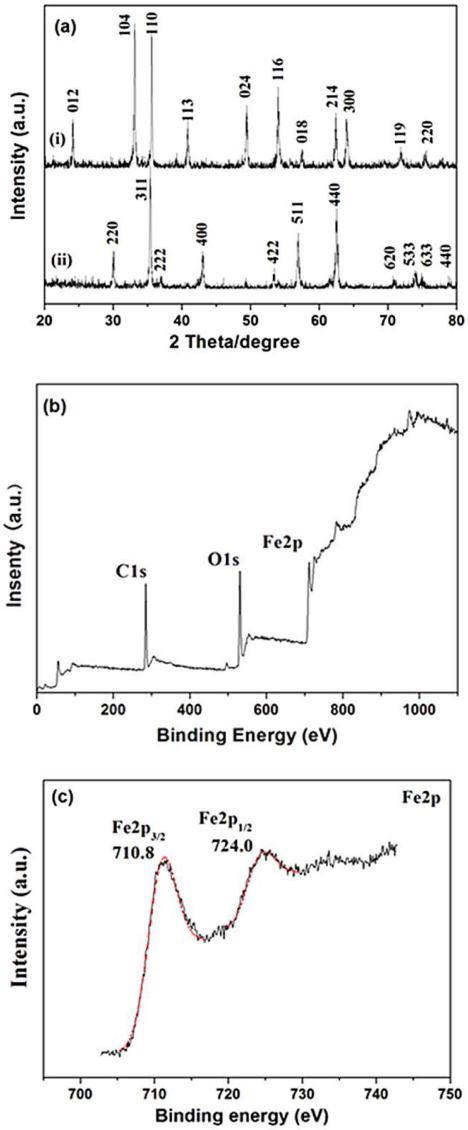

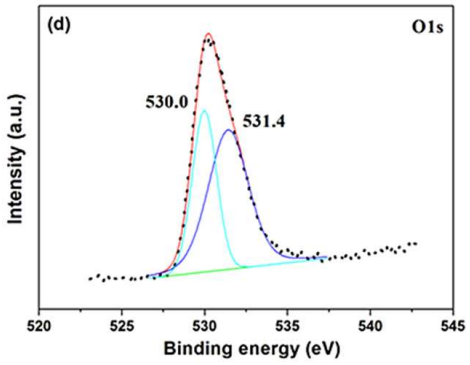

Figure 2. (a) XRD spectra of (i) as-prepared cubic particles by the hydrothermal method, (ii) submicrometer spheres after irradiation with a 248 nm KrF excimer laser for 60 min. (b~d) XPS spectra of submicrometer spheres (b) wide scan, (c) Fe_{2p} spectra, and (d) O_{1s} spectra.

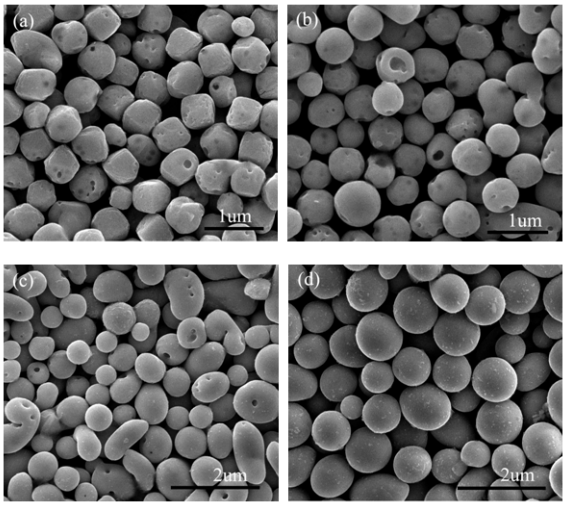

Figure 3. SEM images of the product after irradiating Fe_2O_3 cubic particles by a laser with different fluences for 55 min, (a) 400 mJ pulse^{-1}cm^{-2}, (b) 700 mJ pulse^{-1}cm-^{2}, (c) 1000 mJ pulse^{-1}cm^{-2} and (d) 1300 mJ pulse^{-1}cm^{-2}.

is increased to 0.7 J pulse^{-1}cm^{-2}, all particles exhibit morphologies different from those of the original ones. A number of small particles transform to spheres (Figure 3b). When the laser fluence is further increased, the melting of the particle surfaces and then merging of different particles are clearly exhibited, as shown in Figure 3(c). α-Fe_2O_3 particles change gradually from cube morphology to regular spherical particles when the laser energy density is further increased to 1300 mJ pulse^{-1}cm^{-2} (Figure 3d). This indicates that lasers with proper higher fluence are necessary for submicrometer sphere formation. Moreover, during the particle shape transformation and coalescence processes, the volume of the particle(s) remains constant but the surface areas decrease in comparison with the original particle(s). Therefore, the high surface energy (E_S) of particles is released as EST is proportional to the surface area.

Figure 4 further reveals the morphology evolution of α-Fe_2O_3 particles with irradiation time for the same laser fluence (1.3 J pulse^{-1}cm^{-2}). As the applied laser energy density is high enough to melt the particles, some cubic particles begin to lose their straight edges after 10 min laser irradiation, as shown in Figure 4(a). Quasi-spherical particles emerge after 25 min irradiation, as shown in Figure 4(b). Meanwhile, particle merging is also observed, i.e. several particles begin conjugating into bigger ones. While further prolonging laser irradiation, spherical Fe_3O_4 particles are formed, as shown in Figs. 4(c) and (d). Both particle rounding and coalescence reduce their surface area and, accordingly, the release of the surface energy.

3.3 Mechanisms of morphology evolution and phase transformation. The results above indicate that the reshaping and phase transformation of particles can be delicately controlled by laser fluence and irradiation time. Both are conducted during pulsed laser irradiation, which experiences typical extreme non-equilibrium conditions in nature like high temperature (10^4 K), high pressure (1 Gpa), and high kinetic energy (1 eV).[37] The particle morphology change is

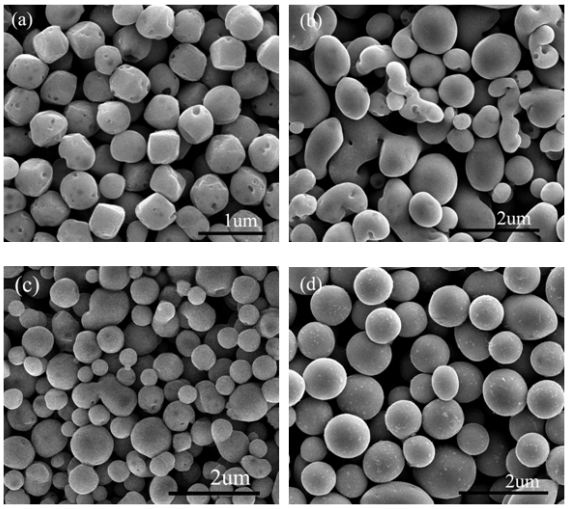

Figure 4. SEM images of the product after irradiating Fe_2O_3 cubic particles with a laser fluence of 1300 mJ pulse^{-1}cm^{-2} for different times: (a) 10 min; (b) 25 min; (c) 40 min; and (d) 55 min.

due to the high temperature of the particle surface caused by laser irradiation. The key feature of micro/nanoparticles is the high surface area per mass (of order 50-300 m^2/g) and one of the consequences of this intrinsic characteristics is the high surface energy concentrated in the surface layers of the particles.[23] The surface energy is proportional to the surface area and can be released by minimizing the surface area. Therefore, the spherical structure has the smallest surface area among all surfaces enclosing a given volume and, accordingly, smallest E_S for spherical particles. Therefore, the pulsed laser irradiation induced heating causes a thermal instability (melting) of the α-Fe_2O_3 cube particle surfaces, cube particles change into spheres gradually with E_S release, as schematically shown in Figure 5. At the same time, since a laser with pulse duration of 25 ns was used, rapid quenching

happened in water after pulsed heating. This is helpful to inhibit the reorientation of surface atoms on a spherical particle, and, finally the particles retained the overall spherical morphology. Moreover, if the surface atoms are activated by laser irradiation above the inter-particle surface potential barrier, contacting particles begin to merge (Figure 3c, 4b) as the surface area of one unified particle is smaller than that of two original individual particles, as shown in Figure 5(b). The particle shape change can thus be well described with the above proposed laser stimulated surface energy release growth mechanism. This method is different from the traditional pulsed laser ablation in liquid, in which particle formation is due to the condensation of laser ablated plasma plumes. [6]

The above results including SEM, XRD and XPS analysis indicate that the α-Fe2O3 particle reshaping was mainly due to the high temperature and high cooling rate involved in pulsed laser irradiation. Meanwhile, electrons can also be generated in water under such extreme non-equilibrium conditions.[38] The Fe_2O_3 particles get these electrons and then release oxygen ions simultaneously, as shown in Figure 5(c). Some of the Fe^{3+} ions in the lattice were thus reduced to

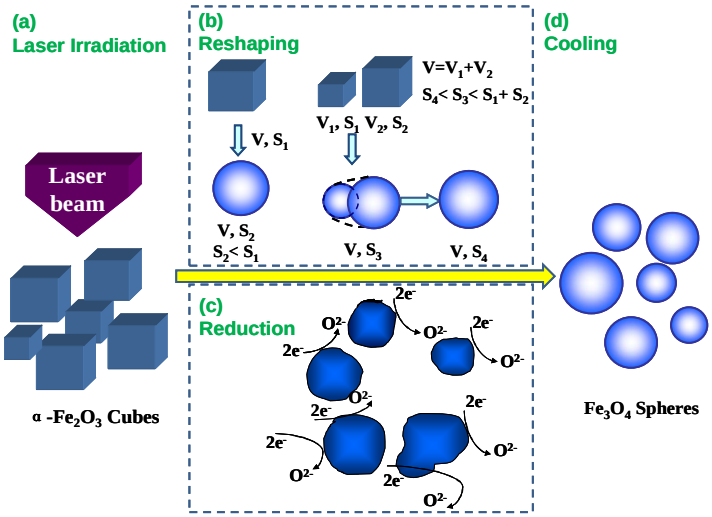

Figure 5. Schematic demonstration of the pulsed laser induced reshaping (b) and reduction (c) mechanism.

Fe^{2+} ions to maintain electroneutrality. Two oxygen ions may recombine to form an O_2 monomer with electron released. These released electrons bound by other Fe_2O_3 particles finally transformed all Fe_2O_3 particles into Fe_3O_4. This process can be simply described by the two chemical reactions (1) and (2). Therefore, the transformation between these two iron oxides is thought to be determined by the diffusion of Fe^{2+} and Fe^{3+} ions within the oxygen sublattice and electron transfer between different valences of Fe ions.[39-41]

$$3Fe_2O_3 + 2e^- \longrightarrow 2Fe_3O_4 + O^{2-} \qquad (1)$$

$$O^{2-} + O^{2-} \longrightarrow O_2 + 4e^- \qquad (2)$$

3.4 Fe_3O_4 submicrometer spheres with enhanced tribology performance. Inspired by their spherical shape and smooth surfaces, the tribology properties of Fe_3O_4 submicrometer spheres (shown in Figure 1b) were measured by adding them in commercial lubricant oils in terms of friction coefficients and diameters of wear scar, while taking cubic submicrometer particles (Figure 1a), nanoparticles (Figure S1a) and microparticles (Figure S2a) as control samples. Figure 6 shows the variation of friction coefficients with time when the commercial pristine lubricating oil (Curve marked with 0wt%) and lubricating oil with α-Fe_2O_3 cube particles (Fig. 6a) or Fe_3O_4 submicrometer spheres (Fig. 6b) as additives are measured with a four-ball tribology tester. It can be seen that the friction coefficients increase obviously when Fe_2O_3 cubic submicrometer particles (0.03 ~ 0.2 wt%) are added into commercial lubricating oil. The reason is that Fe_2O_3 particles with cubic morphology depositing onto the thrust-rings increase the sliding friction. However, when a

certain amount of Fe_3O_4 submicrometer spheres are added into lubricating oils, the friction coefficients apparently decrease. The friction-reduction properties show a clear dependence on the concentration of Fe_3O_4 spherical particles, as shown in Figures 6(a). The friction coefficients decrease when the concentration is smaller than 0.15 wt%. However, the friction coefficients begin to increase when the Fe_3O_4 concentration is larger than 0.2 wt%. Therefore, when the amounts of submicrometer spheres reach an optimal concentration, obvious friction-reduction effect is acquired.

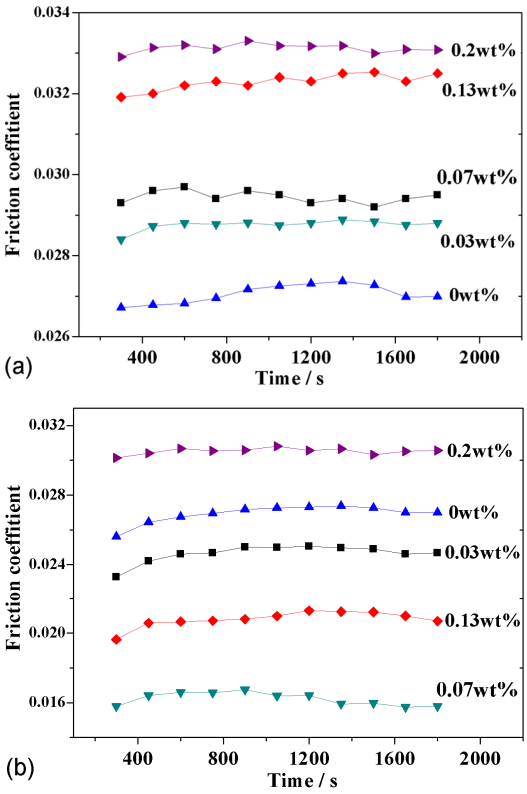

Figure 6. Friction coefficient curve measured with a four-ball tester when particles of different mass concentration were added into the tested oil, respectively, (a) as-prepared Fe_2O_3 cubes and (b) submicrometer spherical Fe_3O_4 particles The friction coefficient measured with pure commercial lubricating oil (curve marked with 0wt%) is also shown for comparison.

For Fe_3O_4 spherical particles, when the sphere concentration is 0.07 wt%, the average friction coefficient decreases by about 38%, which is much more significant than other reported reduction data (<20%).[42]

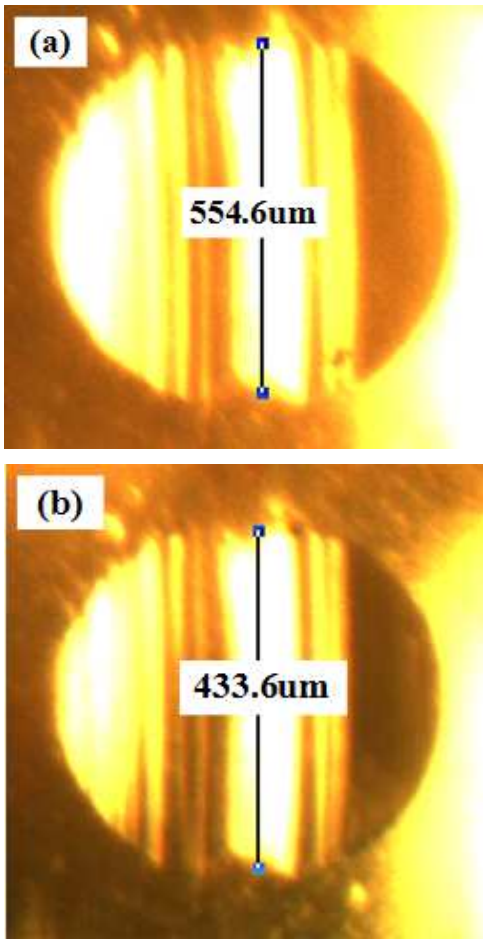

Figure 7. Wear scar images after the four ball test. (a) Lubricated with pure oil and (b) lubricated with oil involving 0.07 wt% Fe_3O_4 submicrometer spheres.

Anti-wear ability is another important characteristic index for lubricant property. Therefore, the wear scar diameter (WSD) was also measured during tribological tests. A metallographic microscope was used to investigate the anti-wear property of different lubricating oils. Figure 7 compares two typical wear scar images of the testing balls in lubricant oil and oil with 0.07 wt% Fe_3O_4 submicrometer spheres, showing a clear decrease of the WSD. Table 1 compares the average wear scar diameters on the testing balls lubricated by lubricant oil dispersions of submicrometer cubic particles and spheres with different mass concentrations. Due to the intrinsic high hardness, both of the particles exhibit anti-wear properties under optimized concentrations, which is similar to that of Al_2O_3 nanoparticles.[25,43] The lubricant oil dispersion with 0.07 wt% Fe_3O_4 spheres performs the most effective, i.e. with WSD reduced by 22%. Similar to the friction-reduction effect, higher concentration of Fe_3O_4 submicrometer spheres or cubic particles (e.g. 0.2 wt%) will deteriorate the anti-wear performance. The maximum decrease of the average friction coefficient and WSD is about 38% and 22%, respectively, when an optimized concentration of Fe_3O_4 submicrometer spheres reaches 0.07 wt%.

Further control experiments reveal that nanoparticles and microparticles could not reach such good tribology performance from submicrometer spheres. The friction coefficients decreased when Fe_3O_4 NPs were added into lubricating oil and the average friction coefficient is smallest when the concentration is 0.1 wt%. But the average friction coefficient decreases by only about 10% (Figure S1b), which is much smaller than for the Fe_3O_4 submicrometer spheres (38%) reported in the paper. Moreover, the best WSD reduction (10%) is also smaller than that of submicrometer spheres (22%), as seen in Table S1. In comparison with the submicrometer Fe_3O_4 spheres, all friction coefficients (Figure S2b) and WSD (see Table S2) increased when Fe_3O_4 microparticles were added into commercial lubricating oil.

The exact mechanism of nanoparticle action as lubricant for enhancing tribological performance is still not very clear.[24,43,44] Basically, inorganic particles are expected to serve as spacer and form a lubrication film when dispersing them in lubricant oils.[40] With the oil is flowing during friction, the nanoparticles can stay between the rubbing surfaces. The existence of nanoparticles on the thrust-ring surface acting as spacer to reduce the friction between the thrust-rings has been identified with SEM and energy-dispersive X-ray spectrum.[43] When the shape of the Fe_3O_4 particles is spherical, the friction between thrust-rings will change from sliding friction to rolling friction using the spheres as molecular bearings.[44,46] As a result, the friction coefficients reduce prominently, as shown in Figure 6(b). But the Fe_2O_3 particles with cube shapes have no such effect and play a negative role on friction reduction, leading to the friction coefficient increase. Therefore, the friction performance of lubricating oil with different Fe_3O_4 submicrometer sphere concentrations can be primarily understood. When the concentration of Fe_3O_4 spheres is low, a small amount of spherical particles starts to play the role of rolling friction instead of sliding friction, which explains well the decrease of the friction coefficients when the additive concentration increases. However, if the concentration of spheres is too high, the redundant spheres will aggregate and chemically condense, which severely enhances friction. Therefore, there is an optimal concentration of submicrometer spheres for lubrication, e.g.0.07 wt% for Fe_3O_4 spheres in our study.

The enhanced anti-wear performance of lubricating oil can be explained with the self-repairing mechanism for lubricant oils containing inorganic particles.[46-47] Fe_2O_3 or Fe_3O_4 particles deposited onto the worn steel surface under compressive stress during the friction process could form a protective film and act as spacers between two friction counterparts. It prevents the metal-to-metal direct contact and fills the wearing scars. In this case, the high hardness of iron oxide is an intrinsic characteristic of the anti-wear application. But the anti-wear ability is also affected by the particle concentration, and, when the Fe_3O_4 microsphere additive concentration reached 0.07 wt%, a better anti-wear performance of lubricant oil in terms of WSD was obtained.

4. CONCLUSIONS

In summary, a novel submicron-sized lubricant based on crystalline iron oxide spheres is demonstrated in this paper revealing that optimized tribology performance can be acquired when lubricant particles are spherical and submicrometer sized. The magnetite submicrometer spheres have been synthesized by laser irradiation hematite cubic

Table 1. Wear scar diameter on the testing balls lubricated with different lubricating oil involving Fe_2O_3 cubic (C) particles or Fe_3O_4 submicrometer spheres (S) with different mass concentrations.

Fe_2O_3/Fe_3O_4 concentration / wt%	0	0.03C	0.07C	0.13C	0.2C	0.03S	0.07S	0.13S	0.2S
Average with error/μm	555±4	535±5	504±4	606±3	623±3	532±2	434±5	538±2	583±4
Reduction/%	--	4	9	-9	-12	4	22	16	-5

particles in water via edge rounding and/or coalescence together with a phase transition. Upon laser irradiation, the Fe_2O_3 particle surface was thermally activated (melting) and the high surface energy concentrated in the surface layer will be released when cube particles change into spheres gradually as a result of surface area minimization, during which electrons in water reduce partially Fe^{3+} to Fe^{2+} ions under a transient high temperature process by laser irradiation, leading to a phase transition from α-Fe_2O_3 to Fe_3O_4. Inspired by their high hardness and smooth surface of the magnetite submicrometer spheres, their tribology performance was explored. This showed that the Fe_3O_4 oxide submicrometer spheres, different from Fe_2O_3 cubic particles, can more effectively reduce the friction coefficients and wear scar diameters under an optimized concentration when dispersing them in lubricating oil, which is a typical morphology-dependent tribological application. Control tribology studies on nanoparticles and micrometer particles revealed that the lubricant property can be optimized when the particles sizes are submicrometer scaled. It is also worth noting that the method applying laser irradiation in liquid medium might be conveniently extended to design other oxide spheres, compensating for the shortcomings of traditional chemical methods in preparing these nanomaterials. We thus expect that our study will be of significance to advance studies on submicrometer sphere based mechanical energy saving applications.

ASSOCIATED CONTENT

Supporting Information

Tribology properties of Fe_3O_4 nanoparticles, Fe_3O_4 microparticles with irregular shapes, and Fe_2O_3 particles and their size distribution after irradiation with different energy densities were included in the Supporting Information. This material is available free of charge via the Internet at http://pubs.acs.org

AUTHOR INFORMATION

Corresponding Authors

* Email: Mse_caobq@ujn.edu.cn ;
Hongqiang.Wang@mpikg.mpg.de

Notes

The authors declare no competing financial interest.

ACKNOWLEDGMENT

This work is supported by NSFC (11174112) and Shandong Provincial Science Foundation for Disguised Youth Scholars (JQ201214). The research projects from Ministry of Education, China, are also acknowledged (NCET-11-1027, 213021A). BC thanks the Taishan Scholar Professorship tenured at University of Jinan (TSHW20091007). HW thanks the Humboldt Fellowship.

REFERENCES

(1)Xia, Y. N.; Xia, X. H.; Wang, Y, Xie, S. F. *MRS Bull.* **2013**, 38, 335-344.
(2) Yang, S. K.; Cai, W. P.; Kong, L. C.; Lei, Y. *Adv. Funct. Mater.* **2010**, 20, 2527-2533.
(3) Oh, M. H.; Yu,T.; Yu, S. H.; Lim, B.; Ko, K. T.; Willinger, M. G.; Seo, D. H.; Kim, B. H.; Cho, M. G.; Park, J. H.; Kang, K.; Sung, Y. E.; Pinna, N.; Hyeon, T. *Science* **2013**, 340(6135), 964-968.
(4) Zhang, L.; Blom, D. A.; Wang, H. *Chem. Mater.* **2011**, 23(20), 4587-4598.
(5) Kensuke, A.; Satoshi, A.; Takaaki, T.; Shingo, I.; Satoshi, T.; Hidemi, N. *Chem. Mater.* **2008**, 20(9), 3042-3047.
(6) Hernández Battez, A.; González, R.; Viesca, J. L.; Fernández, J. E.; Fernández, J. M. D.; Machado, A.; Chou, R.; Riba, J. *Wear* **2008**, 265(3-4), 422-428.
(7) Radice, S.; Mischler, S. *Wear* **2006**, 261(9), 1031041.
(8) Hu, X. L.; Gong, H. B.; Wang, Y. Z.; Chen, Q.; Zhang, J.; Zheng, S. H.; Yang, S. K.; Cao, B. Q. J. *Mater. Chem.* **2012**, 22, 15947-15952.
(9) Zhou,G. H.;Zhu,Y. F.; Wang,X. M.; Xia,M. J.; Zhang, Y.; Ding, H. Y. *Wear* **2013**, 301(1-2), 753-757.
(10) Cao, S. W.; Zhu, Y. J.; Ma, M. Y.; Li, L.; Zhang, L. J. *J. Phys. Chem. C* **2008**, 112(6), 1851-1856.
(11) Peng, D. F.; Beysen, S.; Li, Q.; Jian, J. K.; Sun, Y. F.; Jiwuer, J. L. *Particuology* **2009**, 7(1), 35-38.
(12) Visalakski, G.; Venkateswaran, G.; Kulshreshtha, S. K.; Murphy, P. H. *Mater. Res. Bull.* **1993**, 28(8), 829-836.
(13) Pu, Z. F.; Cao, M. H.; Yang, J.; Huang, Y. L.; Hu, C. W. *Nanotechnology* **2006**, 17(3), 799-804.
(14) Woo, K. J.; Lee,H. J.; Ahnm, J. P.; Park, Y. S. *Adv. Mater.* **2003**, 15(20), 1761-1764.
(15) Lu, J.; Jiao, X. L.; Chen, D. R.; Li, W. J. *J. Phys. Chem. C* **2009**, 113(10), 4012-4017.
(16) Bondi, S. N.; Lackey, W. J.; Johnson, R. W.; Wang, X.; Wang, Z. L. *Carbon* **2006**, 44(8), 1393-1403.
(17) Dave, H. A.; Blank, G.; Rijnders, J. H.; Gertjan, M. K.; Rogalla. H. *Appl. Surf. Sci.* **1998**, 127, 633-638.
(18) N. Fukata, T. Oshima, T. Tsurui, S. Ito, K. Murakami, Sci. Technol. *Adv. Mater.* **2005**, 6(6), 628-632.
(19) Munoz, E.; Maser, W. K.; Benito, A. M.; Martinez, M. T.; DelaFuente, G. F.; Maniette, Y.; Righi, A.; Anglaret, E.; J. Sauvajol, L. *Carbon* **2000**, 38(10), 1445-1451.

(20) Zeng, H. B.; Du, X. W.; Singh, S. C.; Kulinich, Sergei A.; Yang, S. K.; He, J. P.; Cai, W. P. *Adv. Funct. Mater*. **2012**, 22, 1333-1353.
(21) Yang, G. W. Prog. Mater. Sci. **2007**, 52(4), 648-698.
(22) Fojtik, A.; Henglein, A. B.; Buns. *J. Phys. Chem .C* **1993**, 97(2), 252-254.
(23) Liu, J.; Liang, C. H.; Xu, G. P.; Tian, Z. F.; Shao, G. S.; Zhang, L. D. *Nano Energy* **2013**, 2, 328-336.
(24) Qin, W. J.; Sun, J.; Yang, J.; Du, X. W. *Mater. Chem. Phys.* **2011**, 130(1-2), 425-430.
(25) Hu, X. L.; Gong, H. B.; Xu, H. Y.; Wei, H. M.; Cao, B. Q.; Liu, G. Q.; Zeng, H. B.; Cai, W. P. *J. Am. Ceram. Soc.* **2011**, 94(12), 4305-4309.
(26) Zeng, H. B.; Cai, W. P.; Li, Y.; Hu, J. L.; Liu, P. S. *J. Phys. Chem. B* **2005**, 109(39), 18260-18266.
(27) Zeng, H. B.; Yang, S. K.; Cai, W. P. *J. Phys Chem. C* **2011**, 115(12), 5038-5043.
(28) Yang, S. K.; Cai, W. P.; Zeng, H. B.; Xu, X. X. J. *Mater. Chem.* **2009**, 19, 7119-7123.
(29) Yang, S. H.; Kiraly, B.; Wang, W. Y.; Shang, S. L.; Cao, B. Q.; Zeng, H. B.; Zhao, Y. H.; Li, W. Z.; Liu, Z. K.; Cai, W. P.; Huang, T. J. *Adv. Mater.* **2012**, 24, 5598-5603.
(30)Yang, S. H.; Cai, W. P.; Zhang, H. W.; Xu, X. X.; Zeng, H. B. *J. Phys. Chem. C* **2009**, 113, 19091-19095.
(31) Jayawardena, K. D. G. I.; Opoku, C.; Fryar, J.; Silva, S. R. P.; Henley, S. Appl. Surf. Sci. **2011**, 257(12), 5274-5277.
(32) Wang, H. Q.; Kawaguchi, K. J.; Pyatenko, A.; Li, X. Y.; Warkocka, Z. S.; Katou, Y.; Koshizaki, N. *Chem. Eur. J.* **2012**, 18, 163-169.
(33) Wang, H. Q.; Koshizaki, N.; Li, L.; Jia, L. C.; Kawaguchi, K. J.; Li, X. Y.; Alexander, P.; Zaneta, S. W.; Bando, Y.; Dmitri, G. *Adv. Mater.* **2011**, 23(16), 1865-1870.
(34) Ni, Y. H.; Ge, X. W.; Zhang, Z. C.; Ye, Q. *Chem. Mater.* **2002**, 14(1), 1048-1052.
(35) Zhang, D. H.; Liu, Z. Q.; Han, C.; Li, B.; Stewart, M. P.; Tour, J. M.; Zhou, C. W. *Nano Lett.* **2004**, 4, 2151-2155.
(36) Fujii,T.; Groot, F. M. F.; Sawatzky, G. A.; Voogt, F. C.; Hibma, T.; Okada, K.; *Phys. Rev. B* **1999**, 59, 3195-3202.
(37) Liu, Q. X; Yang, G. W.; Zhang, J. X. *Chem. Phys. Lett.* **2003**, 373(1-2), 57-61.
(38) Zhang, H. M.; Liang, C. H.;Tian, Z. F. J. *J. Phys. Chem. C* **2010**, 114(29), 12524-12548.
(39) Jozwiak, W. K. Kaczmarek, E.; Maniecki, T.P.; Ignaczak, W.; Maniukiewicz, W. *Appl. Catal. A. Gen.* **2007**, 326(1), 17-27.
(40) Watanabe, Y. I.; Kuniyoshi, N.; Ishikawa, K.; Furuya,J.; Kato, M. *J. Phys.: Condens. Matter.* **2002**, 14(49), 13643-13651.
(41) Wimmers, O. J.; Arnoldy, P. J.; Moulijn, A. *J. Phys. Chem.* **1986**, 90(7), 1331-1337.
(42) Hernández Battez, A.; Viesca, J. L.; González, R.; Blanco, D.; Sedegbega, E. A.; Osorio, A. *Wear* **2010**, 268(1-2), 325-328.
(43) Shi, G.; Zhang, M. Q.; Rong, M. Z.; Bernd, W.; Klaus, F. *Wear* **2004**, 256(11-12), 1072-1081.
(44) Hernandez Battez, A.; Fernandez Rico, J. E.; Navas Arias, A.; Viesca, J. L.; Rodriguez, A.; Rodriguez, R. C.; Diaz Fernandez, J.M. *Wear* **2006**, 261(3-4), 256-263.
(45) Zhang, B.S.; Xu, B. S.; Xu, Y.; Gao, F.; Shi, P. J.; Wu, Y. X. *Tribol. Int.* **2011**, 44(7-8), 878-886.
(46) Kang, X. H.; Wang, B.; Zhu, L.; Zhu, H. *Wear* **2008**, 265(1-2), 150-154.
(47) Song, X. Y.; Zheng, S. H.; Zhang, J.; Li, W.; Chen, Q.; Cao, B. Q. *Mater. Res. Bull.* **2012,** 47 (12), 4305-4310.

TOC graphic

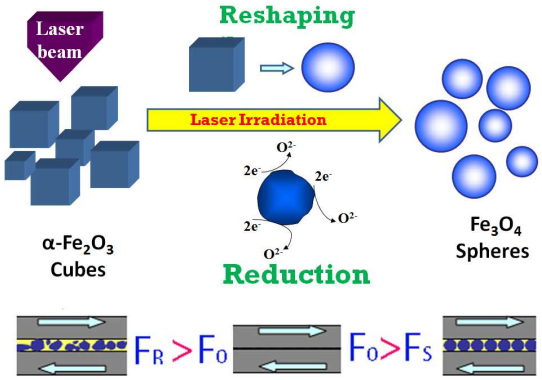
Laser beam
Reshaping
Laser Irradiation
α-Fe2O3 Cubes
Fe3O4 Spheres
Reduction
FR > FO
FO > FS